Electron-Enhanced Hole Injection in Blue Polyfluorene-Based Polymer Light-Emitting Diodes**

By *Teunis van Woudenbergh*, *Jurjen Wildeman*, *Paul W. M. Blom*,* *Jolanda J. A. M. Bastiaansen*, and *Bea M. W. Langeveld-Voss*

It has recently been reported that, after electrical conditioning, an ohmic hole contact is formed in poly(9,9-dioctylfluorene) (PFO)-based polymer light-emitting diodes (PLED), despite the large hole-injection barrier obtained with a poly(styrene sulfonic acid)-doped poly(3,4-ethylenedioxythiophene) (PEDOT:PSS) anode. We demonstrate that the initial current at low voltages in a PEDOT:PSS/PFO-based PLED is electron dominated. The voltage at which the hole injection is enhanced strongly depends on the electron-transport properties of the device, which can be modified by the replacement of reactive end groups by monomers in the synthesis. Our measurements reveal that the switching voltage of the PLED is governed by the electron concentration at the PEDOT:PSS/PFO contact. The switching effect in PFO is only observed for a PEDOT:PSS hole contact and not for other anodes such as indium tin oxide or Ag.

1. Introduction

Since the discovery of polymer light-emitting diodes (PLEDs),[1] it has directly been recognized[2] that charge injection is an important process with regard to their device performance. The charge-injection process may be hindered by the presence of an interface barrier at either the electron or hole contact. Such interface barriers result in an unbalanced charge carrier injection, which gives rise to an excess of one carrier type and consequently a large decrease of the conversion efficiency. Especially for large bandgap materials, as used in blue-emitting PLEDs, large contact barriers may arise.

In order to study the role of an interface barrier on the charge injection into a conjugated polymer, the injection of holes from silver (Ag) into poly(2-methoxy-5-(3′,7′-dimethyloctyloxy)-*p*-phenylene vinylene) (OC_1C_{10}-PPV) has recently been investigated.[3] For this model system the energy barrier for hole injection from Ag into OC_1C_{10}-PPV is typically on the order of 0.9–1 eV,[4] reducing the hole current from Ag into OC_1C_{10}-PPV by 4–5 orders of magnitude as compared to the bulk space–charge-limited current.[3] Subsequently, the role of such a hole-injection barrier on the performance of a PLED has been investigated by incorporating an injection-limited Ag hole contact (anode) in an OC_1C_{10}-PPV-based PLED. At low voltages the limited hole injection in the Ag/OC_1C_{10}-PPV/Ca PLED results, as expected, in a highly reduced current and light output. However, at high applied voltages the current and light output strongly exceed the predictions based on the reduced hole injection, which is attributed to an enhanced electric field near the anode due to the presence of electrons traps near the anode interface.[5]

A widely studied class of polymers for blue PLEDs are the polyfluorenes;[6] a well-known example is poly(9,9-dioctylfluorene) (PFO).[7] The mismatch between the work-function of common electrodes, such as indium tin oxide (ITO) (4.8 eV) and poly(3,4-ethylenedioxythiophene):poly(styrene sulfonic acid) (PEDOT:PSS) (5.2 eV), and the highest occupied molecular orbital (HOMO) of PFO (5.8 eV,[7] 6.1 eV[8]) typically ranges from 0.7–1.1 eV. Therefore, it is expected that the hole current for PFO-based PLEDs is injection limited (IL) due to the presence of an interface barrier between the positive electrode and the HOMO of PFO. As a result the energy band diagram of a PEDOT:PSS/PFO/Ca device (inset of Fig. 1) strongly resembles the diagram of an Ag/OC_1C_{10}-PPV/Ca-based PLED, with a large injection barrier for holes and an ohmic contact for electrons. Studies on the efficiency of the charge injection from PEDOT:PSS into PFO indeed indicate a large reduction (10^{-3}) of the hole current.[7] As a result, it is expected that the IL hole contact will strongly reduce the performance of a PEDOT:PSS/PFO-based PLED. Furthermore, accumulation of electrons at the hole contact has also been observed for PFO from electroabsorption measurements,[9] identical to the interface electron trap in the OC_1C_{10}-PPV IL PLED.

In a recent study it has been demonstrated that the electro-optical characteristics of such a PEDOT:PSS/PFO-based PLED are strongly enhanced upon the first voltage cycle, resulting even in an ohmic contact of PEDOT:PSS on PFO.[10] Furthermore, it has been shown that with an electron-blocking top contact the hole injection is not enhanced, indicating that

[*] Prof. P. W. M. Blom, T. van Woudenbergh, J. Wildeman
Materials Science Centre, University of Groningen
Nijenborgh 4, NL-9747 AG Groningen (The Netherlands)
E-mail: P.W.M.Blom@phys.rug.nl
J. J. A. M. Bastiaansen, Dr. B. M. W. Langeveld-Voss
TNO Institute of Industrial Technology
PO Box 6235, NL-5600 HE Eindhoven (The Netherlands)

[**] This work forms part of the research program of the Dutch Polymer Institute (DPI).

 DOI: 10.1002/adfm.200305178

electrons play a role in the increase of the hole injection. Due to the large bandgap of blue-light-emitting polymers it is very difficult to make an ohmic hole contact using metals or ITO. Therefore, understanding of the mechanism responsible for the enhanced hole injection is important for the design of efficient blue-light-emitting PLEDS.

In this study we focus on the role of the electrons in the switching during the first voltage cycle. It is demonstrated that the low current in the PEDOT:PSS/PFO/Ca PLED (PEDOT PLED) device preceding the switching effect is electron dominated. This electron-dominated current can be manipulated by the reactive end groups on the PFO chain. It is shown that by replacing these end groups with monomer units via end-capping, the electron current can be strongly enhanced. This enhanced electron current is accompanied by a reduction of the voltage required for the switch-on of the device. The dependence of the switching voltage on sample thickness confirms that the effect is governed by the concentration of electrons at the hole injection contact. From impedance spectroscopy measurements it is found that, after switching, typically 10^{17} electrons per square meter have accumulated at the anode interface. Enhancing the electron injection by replacing Al[10] with Ca also leads, as expected, to a strong decrease of the switching voltage. Another important observation is that the enhanced hole injection is specific for the PEDOT:PSS/PFO interface, and does not occur for ITO and Ag bottom contacts. This, together with the observed sharpness of the transition, points to a mechanism in which the trapped electrons give rise to a strong dipole across a thin insulating injection barrier present at the PEDOT:PSS interface. At the moment that the dipole is sufficiently large, holes from the PEDOT:PSS will directly tunnel into the transport states of the PFO, giving rise to a sharp increase of the hole current.

2. Results

2.1. Electro-optical Characteristics of a PEDOT:PSS/PFO/Ca LED

Four types of devices have been investigated, all consisting of a spin-coated layer of the polymer PFO sandwiched between two electrodes (see Experimental). Two of these device types are designed to be bipolar: an ITO/PFO/Ca PLED (ITO PLED) and an ITO/PEDOT:PSS/PFO/Ca PLED (PEDOT PLED). Furthermore, for the investigation of the hole injection, ITO/PEDOT:PSS/PFO/Au hole-only devices have been constructed, with an electron-blocking Au top contact. In order to discriminate whether the current in the ITO PLED and the PEDOT PLED is dominated by the (reduced) hole or the electron current devices, have also been constructed where the ITO bottom contact has been covered by Ag (ITO/Ag/PFO/Ca). Ag has a work function of only 4.3 eV,[4] as compared to the 5.8–6.0 eV of the HOMO of PFO. Therefore, such a device is expected to be completely dominated by the electron current that is injected from the Ca top contact (electron-only device). For these four types of devices direct current (DC) current density–voltage (J–V), impedance, and transient electroluminescence measurements have been performed.

Figure 1a shows a current density–voltage (J–V) measurement for a "fresh" PEDOT PLED (i.e., electrically addressed for the first time). It is observed that this plot strongly resem-

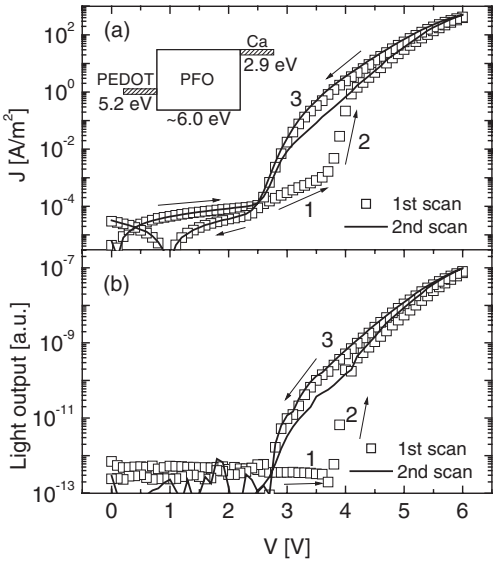

Figure 1. Current density–voltage (J–V) characteristics of an ITO/PEDOT:PSS/PFO/Ca/Al PLED (PEDOT PLED) at room temperature (a), together with light output (b). The squares show the first electrical addressing and solid lines correspond to the second cycle. The thickness of the active layer is $d = 85$ nm. The inset shows the energy diagram for such a PEDOT PLED. The numbers 1, 2, and 3 mark the different regimes in the plot.

bles the electrical characteristics as shown by Poplavskyy et al.[10] A remarkable difference is the very low switching voltage V_{switch}, due to the thin film and the ohmic Ca contact.

The electrical characteristics in Figure 1a can be divided in three regimes: In regime 1, a strongly reduced current is observed. In this regime, the hole current is negligible and the current is carried by electrons. From the absence of light output in regime 1 it is also observed that the current is unipolar. Then, at a voltage V_{switch} of typically 3–4 V, a sudden transition is observed and the current increases by several orders of magnitude (regime 2). Concurrent with the transition of the current from low to high, also the light output of the device switches on (Fig. 1b). When the voltage is further increased and subsequently decreased towards zero the current stays in this on-state (regime 3). For subsequent voltage cycles the current follows the high regime (solid lines in Figs. 1a,b). For the receding J–V curve a small dip is observed. This has been observed before by Riess et al.[11] in NPB/Alq_3 systems (where Alq_3 is tris(8-hydroxyquinoline) aluminum) and is explained by release of charge from deep traps.

For applications it is relevant to know whether the observed switching effect is permanent, for example, due to a chemical reaction at the interface. Then the PFO-based PLED has to be programmed only once before it is used. However, as shown in

ADVANCED FUNCTIONAL MATERIALS

Figure 2, the on-state of the device is not permanent. Over a long period of time, the PEDOT PLED tends to return to its original off-state. Sixteen days after the initial switching of the

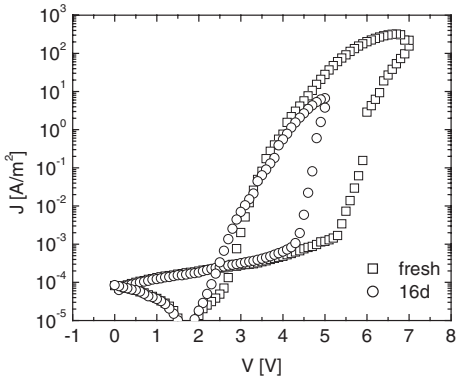

Figure 2. *J–V* characteristics as a function of time at room temperature. Thickness d =100 nm. The very first *J–V* curve (fresh) is shown, together with the *J–V* curve after 16 days. After the fresh *J–V* scan a subsequent *J–V* scan was made to ensure the on-state is obtained (not shown).

device to its on-state, the device follows the low current of regime 1 for low voltages, and switches at $V_{switch} \sim 4.5$ V. From Figure 2 it can be estimated that full recovery of the off-state takes ~1 month (~10^6 s) at room temperature (RT); this is subject of further study.

2.2. Regime 1: Electron-Dominated *J–V* Characteristics

In order to understand the switching effect, first the origin of the low current in regime 1 is investigated. It is demonstrated that the low current in regime 1 is also observed for an ITO PLED and an ITO/Ag/PFO/Ca (electron only) device, as shown in Figure 3.

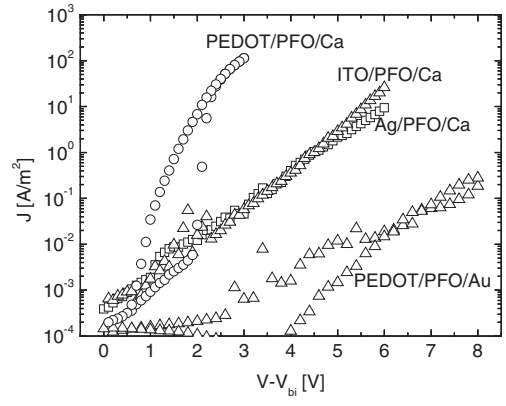

Figure 3. *J–V* characteristics of a PEDOT PLED, together with the current density of an ITO/PFO/Ca/Al PLED (ITO PLED), an ITO/Ag/PFO/Ca/Al device (electron-only), and an ITO/PEDOT:PSS/PFO/Au device, all with thickness d = 80 nm. The applied bias is compensated for the built-in voltage, V_{bi}. For the PEDOT PLED and for the ITO PLED V_{bi} = 2 V, and for the electron-only V_{bi} = 1 V. The ITO/PEDOT:PSS/PFO/Au device has a negligibly small built-in voltage.

Since at low voltages the current density for the PLEDs with a PEDOT, ITO, or Ag anode are equivalent it is concluded that the electron current is dominant in these devices. A contribution from the hole current would give a large difference in current between these devices, as the hole-injection barrier amounts to 0.7 eV for PEDOT, 1 eV for ITO, and 2 eV for Ag. This is confirmed by a direct measurement of the IL hole current from PEDOT:PSS. Furthermore, it is observed that the hole current does not switch on in the devices with an ITO or Ag bottom contact.

It is observed that for a PEDOT:PSS/PFO/Au device, where the electron injection is blocked, the injection-limited hole current from PEDOT:PSS is 2–3 orders of magnitude smaller than the electron current. Furthermore, it demonstrates that the IL hole current is 5–6 orders of magnitude below the on-state current of the PEDOT PLED. This indicates the presence of a large injection barrier of PEDOT:PSS on PFO. Furthermore this measurement confirms that the switching effect is not observed for a PEDOT PLED with an electron-blocking Au contact, as was already mentioned by Poplavskyy et al.[10]

Knowing that the current in regime 1 is electron dominated enables us to further investigate the role of electrons in the switching effect. Apart from modifying the electron current by a change of the cathode (Au versus Ca) it is found that the electron current can also be modified by a specific step in the synthesis of PFO. The presence of reactive end groups, required for the polymerization, strongly influences the magnitude of the electron current. In Figure 4a the reaction scheme is shown for three different syntheses of PFO. PFO(1) still contains both the reactive end groups whereas in PFO(2) and PFO(3) one of the reactive end groups has been replaced by mono-functionalized fluorene or benzene. Adding end-capping reagent during the polymerization will reduce the molecular weight and give rise to variations in polymer length.[12] Therefore, end-capping is performed after polymerization has been finished. From gel permeation chromatography (GPC) it is found that the molecular weight for the three polymers PFO(1–3) is typically 30 000 g mol^{-1}.

It has already been found that end-capping has a strong influence on the electroluminescence of PF2/6, a similar polyfluorene.[12] This has been attributed to aggregates in the original non-end-capped polymer. Here we show that end-capping has a major influence on the electron transport. In Figure 4b the electrical characteristics of PEDOT PLEDs via each of these three PFO synthesis routes is shown. The devices have all been made within one process run to exclude processing variations. It is directly observed that the current in regime 1 is strongly dependent on the reaction scheme followed. For PFO(1), where the reactive end groups are still present, the electron current is very low. For PFO(2), where the Br end group has been replaced by a fluorene monomer, and PFO(3), which has been end-capped with a phenyl group, the electron current is much higher.

For the three PFO types, electroluminescence (EL) spectra have also been recorded. It is observed that for higher current densities the contribution of blue light becomes higher, as has been observed in the literature.[12] For a fair comparison, the

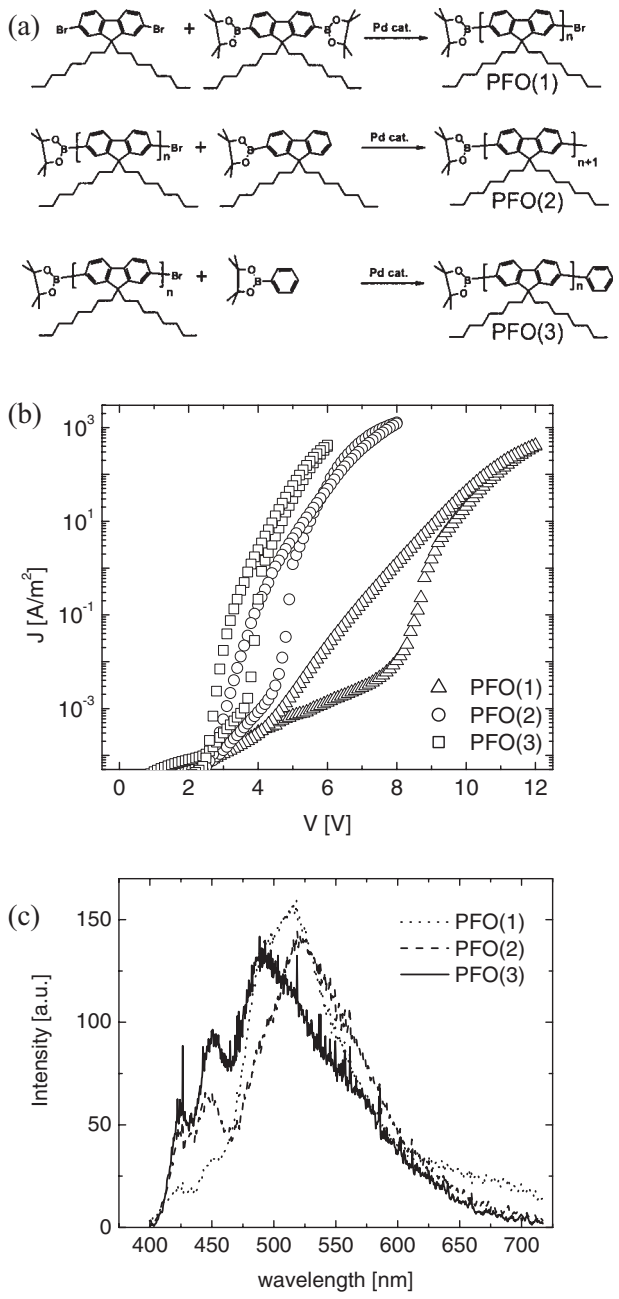

Figure 4. a) The basic synthesis of 9,9-dioctyl-PF according to Miyaura and Suzuki [13], resulting in PFO(1), together with end-capping with the 9,9-dioctyl-fluorene monomer (PFO(2)) and the benzene monomer (PFO(3)). b) *J–V* characteristics of the three polymers, with thicknesses $d = 90$ nm for PFO(1), $d = 105$ nm for PFO(2), and $d = 85$ nm for PFO(3). c) EL spectra for the three polymers, normalized to their integrated intensity.

EL spectra are recorded at a constant current density ($\sim 10^3$ A m^{-2}). From the EL spectra (Fig. 4c) it is observed that PFO(1) is dominated by green emission (maximum 520 nm), while the end-capped PFO(2) shows both a blue (430 nm, 450 nm) and a green component (530 nm). PFO(3) has no green emission, but three blue/blue–green peaks (420 nm, 450 nm, 500 nm). It is also observed that the EL spectra do not change for subsequent electrical conditioning.

2.3. Regime 2: Switch-on

From Figure 4b it is observed that the switching voltage V_{switch} is lowered when the electron current is higher. Clearly, a larger electron current will result in a stronger accumulation of electrons at the hole-injecting contact. In order to discriminate whether it is the electron current or the electron concentration at the anode that dominates the switching effect, the effect of sample thickness on switching voltage has been studied.

Using PFO(3), the switching voltage as a function of thickness is plotted in Figure 5. It is observed that the switching voltage scales with the square of the thickness (solid line). For space–charge-limited charge transport, the concentration of

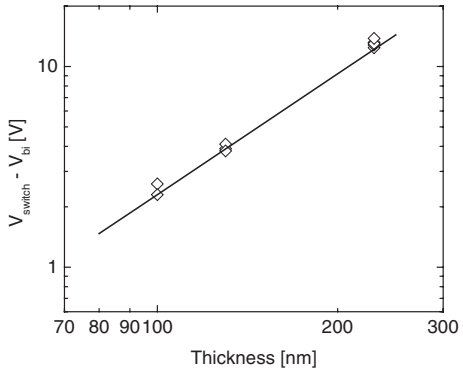

Figure 5. Thickness dependence of the switching voltage V_{switch}, compensated for the built in voltage V_{bi}. The solid line corresponds to quadratic behavior (slope 2).

electrons at the anode (distance L from the cathode) scales with thickness as[14] $n(L) \propto V/L^2$. Consequently, the observed quadratic scaling with L demonstrates that all devices switch when the electron concentration at the anode reaches a certain value. This implies that the switching is governed by the amount of (trapped) electrons at the anode.

A very useful technique for analyzing charge concentrations at interfaces is impedance spectroscopy (IS).[15] With this technique, the real and imaginary part of the impedance is measured as a function of frequency. From the impedance scan the different charge layers can be separated by treating them as equivalent resistance–capacitance (RC) circuits. In Figure 6 the real and imaginary parts of the impedance are plotted in an *xy*-graph with the frequency as a parameter ($f = 20$ Hz–1 MHz). Figure 6 shows IS for a fresh PEDOT PLED, where Figure 6a is at $V = 3$ V, characteristic for $V \leq 3$ V, and Figure 6b is for $V = 3.2$ V. For $V \leq 3$ V, one large semicircle is observed, corresponding to one charge layer with a large differential resistance. Modeling this device as a parallel RC circuit (inset Fig. 6a) gives a (differential) capacitance $C_1 = 2.3$ nF, which is in agreement with the geometrical capacitance using $\varepsilon_r = 2.1$. At a slightly higher voltage, $V = 3.2$ V, the device starts to switch on, as has been observed from the photodiode current during the IS measurement. As shown in Figure 6b at $V = 3.2$ V a clear double semicircle is observed. Modeling the

ADVANCED FUNCTIONAL MATERIALS

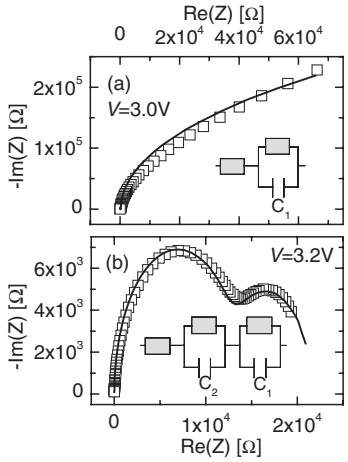

Figure 6. Impedance spectroscopy (IS) of a PEDOT PLED with thickness $d = 80$ nm at room temperature. Measurements are shown for an applied bias of a) $V = 3$ V and b) $V = 3.2$ V. The solid lines are fits from the equivalent circuits (insets).

device as a double RC circuit (inset of Fig. 6b), capacitance values of $C_1 = 2.1$ nF and $C_2 = 70$ nF are obtained for $V = 3.2$ V.

Despite the large difference in impedance for $V = 3$ V and $V = 3.2$ V, the values of the capacitance C_1 are quite close. This shows that C_1 is the bulk capacitance and that C_2, which is only observed clearly above 3 V, must definitely be related to the switching effect. Similar observations have also been reported by Poplavskyy et al.[10]

In order to investigate the relation between this extra RC circuit and the switching effect, a complete voltage sweep was made. The differential capacitances C_1 and C_2 have been plotted in Figure 7. It is observed that C_1 does not depend on bias, as is expected for the geometrical capacitance. However,

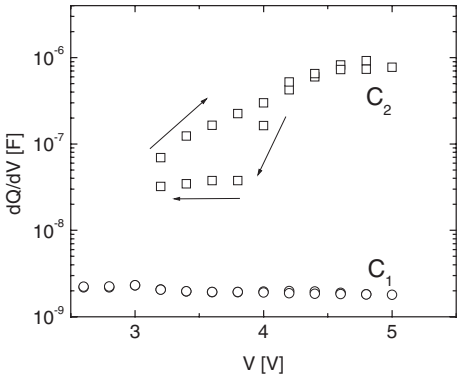

Figure 7. Differential capacitances C_1 and C_2 as a function of applied bias. Capacitance C_1 is the bulk capacitance and the component C_2 corresponds to the charge layer at the interface between PEDOT:PSS and PFO.

C_2, which is attributed to charging of the PEDOT:PSS/PFO interface, strongly depends on the applied voltage and increases up to 1 μF at 5 V (Fig. 7) As a consequence, a lot of charge is built up during the voltage scan. Decreasing the voltage again, C_2 sharply decreases meaning that the charge that is accumulated at high voltage is trapped at the PEDOT:PSS/PFO interface.

The amount of charges at the PEDOT:PSS/PFO interface, N_i, can be calculated by integrating the differential capacitance C_2 as a function of voltage (Eq. 1):

$$N_i = \frac{1}{eA}\int_0^V C_2 \mathrm{d}V \tag{1}$$

As the voltage over C_2 does not equal the applied bias, it has been corrected by integrating the differential resistances of both circuits and finding the voltage drop over each circuit separately. The surface charge N_i, calculated from Equation 1 is plotted in Figure 8.

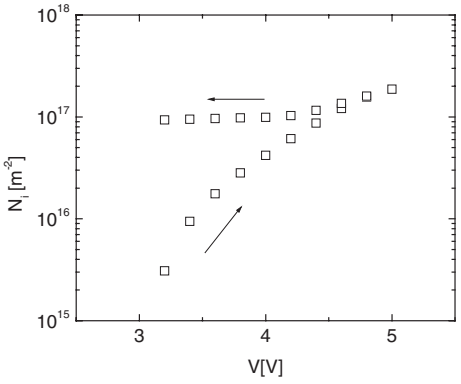

Figure 8. Surface charge density N_i (Eq. 1) found from C_2 (Fig. 7) for a PEDOT PLED.

Looking in more detail, Figure 8 also contains three regimes. At small voltages on the advancing curve, charge is being built-up super-linearly. Then, at ~4 V, saturation takes place ($\mathrm{d}Q/\mathrm{d}V$ is approximately constant, Fig. 7), and C_2 behaves as a normal capacitor with a high capacity. For voltages < 4 V on the receding curve, excess charge remains at the interface. It is observed that the trapped surface charge concentration amounts to $N_{it} = 1 \times 10^{17}$ m^{-2}. This is of the same order of magnitude as $N_{it} = 2 \times 10^{16}$ m^{-2} observed[5] at a Ag/OC$_1$C$_{10}$-PPV interface. These numbers show that a high interface density is required to enhance the hole injection.

2.4. Regime 3: On-state

In order to confirm whether the electro-optical characteristics of the PEDOT PLED in this regime are bulk limited[10] (implying ohmic contacts), or still limited by the hole injection, we have measured the hole mobility with transient electroluminescence[16] (TEL). From our measurements we find a zero-field mobility $\mu_0 = 1.0 \times 10^{-9}$ m^2/V s and a field prefactor $\gamma = 5.5 \times 10^{-5}$ (m/V)$^{1/2}$. The corresponding space–charge-limited current is in close agreement with the experimentally observed J–V characteristic, showing that the current in the PLED after switching is indeed bulk limited.

3. Discussion

The formation of an ohmic hole contact on PFO has been attributed to trapped electrons that increase the electric field at the anode and consequently enhance the hole injection.[10] This mechanism had been recently proposed to explain the current enhancement in OC_1C_{10}-PPV-based LEDs with a limited hole injection from a Ag contact.[5] However, there are a number of fundamental differences between the behavior of the Ag/PPV and PEDOT/PFO contacts. For OC_1C_{10}-PPV-based PLEDs the enhanced current and light output are observed for different anodes, for example, Ga, In, and Ag.[5] These different anodes have a very different chemical interaction with the polymer and therefore the electron trap in an OC_1C_{10}-PPV-based PLED is not related to the anode material, but is an intrinsic property of the polymer. On the other hand, for PFO the effect of an enhanced current is specifically observed for a PEDOT:PSS anode, and not for contacts such as ITO or Ag. In this case, the electron trap at the interface must be the result of a specific interaction of the PFO and the PEDOT:PSS or related to a specific property of the PEDOT:PSS. Moreover, from the *J–V* characteristics of a PEDOT PLED (Fig. 1) a very sharp transition is observed, whereas the increase in the *J–V* characteristics of an OC_1C_{10}-PPV based PLED is more gradual and does not exhibit any hysteresis.[5] This is in contrast with the PEDOT/PFO PLED where the 'on-state' is maintained with decreasing voltage.

A further indication for the origin of the switching effect is that the switching process is reversible on a long time scale ($\sim 10^6$ s at RT, Fig. 2), which excludes chemical modification of the interface as the origin of the switching behavior. The underlying principle must be physical, e.g., a deep trap. However, a deep trap alone is not sufficient to explain the effect; model calculations on an IL PLED demonstrate that such a trap level is gradually filled with increasing voltage and therefore gives rise to a gradual increase of the current.[5] The sharp transition observed in the first *J–V* scan (Fig. 1) points towards a different mechanism, like the presence of a thin tunnel barrier. Experiments with 3 eV electrons impinging a free PEDOT:PSS film show modification of the chemical compounds at the outermost region of the film, although reported for longer time scale (hours).[17] Experimental evidence is found from X-ray experiments on a PEDOT:PSS layer that shows segregation of the PSS dopant towards the PEDOT:PSS surface, forming a layer of PSSH at the interface of a few nanometers.[18] It might be that this small layer forms a tunnel barrier and is therefore responsible for the sharp transition. In that case, the effect at the PEDOT:PSS/PFO interface is charging of a small insulating layer through which holes must tunnel at a high field. The resulting dipole shifts the Fermi-level of PEDOT:PSS towards the HOMO of PFO and from a certain voltage the holes can directly tunnel into the transport states of the HOMO of PFO. The density of trapped electrons as determined from IS, $N_{it} \sim 10^{17}$ m^{-2}, results in an electric field across the insulating layer of $E \sim 10^9$ V m^{-1}. An insulator thickness of only 1 nm therefore would result in a dipole of 1 V, equal to the difference in work function of PEDOT:PSS and the HOMO of PFO. For poly[(9,9-dioctylfluorene)-*co*-benzothiadole], a polymer similar to PFO, Murata et al.[19] have modeled the device characteristics of a PLED with a PEDOT:PSS anode by including a tunnel barrier at the anode. Their model calculations show that the generated electric field at a tunnel barrier indeed gives rise to a sharp increase of the hole injection.

Finally, we have demonstrated that the electron transport in PFO can be manipulated via the synthesis route. The only difference between the polymers PFO(1), PFO(2), and PFO(3) is the last step, the replacement of one of the reactive end groups of the polymer by a fluorene or benzene monomer via end-capping. It is observed from Figures 4b and 4c that the reduced electron transport is accompanied by an increase of the green 530 nm emission (PFO(1) and PFO(2)). The peak at 530 nm is attributed to emission from chromophores where the side chains have been replaced by a double-bonded oxygen (fluorenone).[20] Apparently, the fluorenone defects serve as efficient electron traps,[20] as indicated by the reduced electron current. The relation between the different end-capping groups and the occurrence of fluorenone defects is a subject of further study. Due to a difference in electron transport the polymers PFO(1–3) also exhibit a different switching voltage, which is controlled by the amount of electrons at the hole-injecting contact.

4. Conclusions

In summary, it is found that the switching of a PFO-based PLED is specific for a PEDOT:PSS hole contact. This can be due to specific properties of the PEDOT:PSS, or to a specific interaction of PEDOT:PSS with PFO, which does not occur for ITO or Ag. Furthermore, the device in the off-state is controlled by electron transport. This electron transport depends strongly on the way the polymer is end-capped. The switching voltage is strongly dependent on the electron current, and it has been found that the electron concentration at the PEDOT:PSS/PFO contact controls the switching voltage of the device.

5. Experimental

Polymer Synthesis: The poly(9,9-dioctylfluorene) (PFO) was synthesized via Suzuki coupling [13]. The polymerization was performed in an inert atmosphere. Monomers are 2,7-bis(4,4,5,5-tetramethyl-1,3,2-dioxaborolyl)-9,9-dioctylfluorene and 2,7-dibromo-9,9-dioctylfluorene. PFO(1) and PFO(2) were synthesized in one single batch. After finishing the polymerization, 4,4,5,5-tetramethyl-1,3,2-dioxaborolyl-9,9-dioctylfluorene (end-capping reagent) and some fresh catalyst were added to a part of the solution to obtain the end-capped PFO(2). For the synthesis of PFO(3), after finishing the polymerization, 4,4,5,5-tetramethyl-1,3,2-dioxaborolylbenzene (end-capping reagent) and some fresh catalyst were added. The polymers were carefully purified to remove catalyst residues. Then, the polymers were dried and isolated. Finally, GPC measurements were performed to determine the molecular weight. For polymers PFO(1) and PFO(2) a molecular weight $M_W = 34\,300$ g mol^{-1} was found, and for PFO(3) the molecular weight amounts to $M_W = 27\,500$ g mol^{-1} (according to polystyrene standards). NMR spectra were taken and found to be identical.

ADVANCED FUNCTIONAL MATERIALS

Device Characterization: The devices were fabricated in a clean-room environment and kept in a nitrogen atmosphere from the moment the polymer layer was spin-coated. Pre-patterned glass/ITO substrates were cleaned by washing in detergent solution followed by baths in acetone and isopropyl alcohol. Subsequently, UV–ozone plasma treatment was performed. Different types of bottom electrodes were used: the bare ITO contact, a contact where the ITO has been covered with PEDOT:PSS (Baytron P, supplied by Bayer AG, Germany), and a bottom contact of ITO covered with Ag. After spin-coating the PFO from toluene a Ca top contact was thermally evaporated. Ca is a good electron injector (work function of Ca ~ 2.9 eV [4]), which is in line with the lowest unoccupied molecular orbital (LUMO) of PFO. In order to block electron injection, a gold (Au) top contact was used (work-function 5.1 eV [4]). Current density–voltage (J–V) measurements were performed using a source measure unit Keithley 2400, and the light output was recorded using a photodiode connected to a Keithley 6514 electrometer. Impedance spectroscopy (IS) measurements were carried out using an Agilent 4284A LCR meter. Moreover, charge-carrier transit times were measured by transient electroluminescence using an Agilent 8114A pulse generator. The electroluminescence data were recorded with an Ocean Optics spectrometer (USB2000).

Received: December 12, 2003

[1] J. H. Burroughes, D. D. C. Bradley, A. R. Brown, R. N. Marks, K. Mackey, R. H. Friend, P. L. Burn, A. B. Holmes, *Nature* **1990**, *347*, 539.

[2] R. N. Marks, D. D. C. Bradley, *Synth. Met.* **1993**, *57*, 4128.

[3] T. van Woudenbergh, P. W. M. Blom, M. C. J. M. Vissenberg, J. N. Huiberts, *Appl. Phys. Lett.* **2001**, *79*, 1697.

[4] I. H. Campbell, T. W. Hagler, D. L. Smith, J. P. Ferraris, *Phys. Rev. Lett.* **1996**, *76*, 1900.

[5] T. van Woudenbergh, P. W. M. Blom, J. N. Huiberts, *Appl. Phys. Lett.* **2003**, *82*, 985.

[6] D. Neher, *Macromol. Rapid Commun.* **2001**, *22*, 1365.

[7] A. J. Campbell, D. D. C. Bradley, H. Antoniadis, *J. Appl. Phys.* **2001**, *89*, 3343.

[8] L.-S. Liao, C. S. Lee, S. T. Lee, M. Inbasekaran, W. W. Wu, in *Conjugated Polymer and Molecular Interfaces* (Eds: W. R. Salaneck, K. Seki, A. Kahn), Dekker, New York **2002**, Ch. 7.3.

[8] P. A. Lane, J. C. de Mello, R. B. Fletcher, M. Bernius, *Appl. Phys. Lett.* **2003**, *83*, 3611.

[10] D. Poplavskyy, J. Nelson, D. D. C. Bradley, *Appl. Phys. Lett.* **2003**, *83*, 707.

[11] W. Riess, H. Riel, T. Beierlein, W. Brütting, P. Müller, P. F. Seidler, *IBM J. Res. Dev.* **2001**, *45*, 77.

[12] T. Miteva, A. Meisel, W. Knoll, H. G. Nothofer, U. Scherf, D. C. Müller, K. Meerholz, A. Yasuda, D. Neher, *Adv. Mater.* **2001**, *13*, 565.

[13] N. Miyaura, A. Suzuki, *Chem. Rev.* **1995**, *96*, 2457.

[14] M. A. Lampert, P. Mark, *Current Injection in Solids*, Academic Press, New York **1970**.

[15] J. R. MacDonald, *Impedance Spectroscopy*, J. Wiley & Sons, New York **1987**.

[16] P. W. M. Blom, M. C. J. M. Vissenberg, *Phys. Rev. Lett.* **1998**, *80*, 3819.

[17] A. W. Denier van der Gon, J. Birgerson, M. Fahlman, W. R. Salaneck, *Org. Electron.* **2002**, *3*, 111.

[18] G. Greczynski, T. Kugler, W. R. Salaneck, *Thin Solid Films* **1999**, *354*, 129.

[19] K. A. Murata, S. Cinà, N. C. Greenham, *Appl. Phys. Lett.* **2001**, *79*, 1193.

[20] E. J. W. List, R. Güntner, P. Scandiucci de Freitas, U. Scherf, *Adv. Mater.* **2002**, *14*, 374.

